Russ. J. Numer. Anal. Math. Modelling, Vol. 26, No. 1, pp. 17–38 (2011)
DOI 10.1515/ RJNAMM.2011.002

Simulation of surface waves generated by an underwater landslide moving over an uneven slope

S. A. BEIZEL*, L. B. CHUBAROV*, and G. S. KHAKIMZYANOV*

Abstract — This paper is focused on the study of the effect of an underwater slope unevenness on the wave mode characteristics caused by the motion of a landslide over this slope. Using the simplest model representation of a landslide in the form of a rigid body, the authors consider two model reliefs, taking to some extent into account the peculiarities of the Mediterranean coast of Israel. The simulation of wave processes is performed within the framework of the equations of the shallow water theory. The results of the comparison of wave modes are discussed, the dependences of the characteristics of these modes on geometric and physical parameters of the studied phenomena, such as the landslide bedding depth, its length and thickness, the geometry of the slope, and the friction force are analyzed.

The interest in studying the landslide mechanism of surface waves generation in coastal water areas is stregthened by a series of catastrophic events that lately took place in different parts of the World Ocean, because the origin of such events is generally connected with such mechanism. The landslide mechanism of tsunami wave generation is called anomalous, in contrast to the traditional seismic one. The anomaly means the discrepancy between an appreciable tsunami wave near the shore and a weak earthquake associated with its generation, which in fact may be only a trigger initiating the landslide mechanism of wave generation. Such anomalous events make up approximately 15% of the registered historical tsunami.

In mathematical modelling, the model of landslide motion, as well as the model of surrounding liquid should be developed. There are known approaches to modelling landslides by the motion of a rigid body [8, 10, 17, 22, 25] or a set of such bodies [20]. Other approaches use the simulation of the landslide mass motion by a flow of liquids differing in their density, viscosity, etc. [12, 14, 20], or by the motion of some elasto-plastic medium with or without taking into account the interaction with the surrounding liquid [7]. In some papers the phenomenon is modeled as the flow of a two-layer liquid with layers having different densities and viscosity coefficients [11, 13, 15].

It was shown in [7, 10, 18, 25] that the simulation of a real landslide by a model rigid body and the choice of an appropriate motion law for it give an adequate de-

*Institute of Computational Technologies, Siberian Branch of the Russian Academy of Sciences, Novosibirsk 630090, Russia

The work was supported by the Russian Foundation for Basic Research (09-05-00294, 06-05-72014) and the Program ‘Leading Scientific Schools of Russian Federation’ (931.2008.9).

scription of the wave process for a wide range of such parameters as the inclination of the flat slope, the thickness and length of the landslide, its initial depth.

The peculiarity of simulation of surface waves generated by a landslide is the fact that these waves originate from a shallow coastal zone, the duration of the landslide is rather large and comparable with the period of the generated wave, and the typical depth and the vertical size of the landslide are also comparable. Therefore, the hydrodynamic aspects of wave processes are studied within the approximate models of wave hydrodynamics. The investigations carried out by the authors earlier allowed us to estimate the efficiency of this class of models by comparing results obtained with the use of those models and materials of laboratory experiments [3]. The comparison was done for the simplest case when the bottom relief was a uniform slope passing into a flat bottom segment. The conclusion made by the authors of the papers mentioned here [2, 3, 6, 19] was that in some particular range of the parameters of the problem, a sufficiently adequate description of the wave modes can be obtained using the simplest shallow water models, whereas a more detailed study requires the involvement of nonlinear-dispersive shallow water models taking into account the non-hydrostatic pressure and, which is the same, taking into account the contribution of the vertical flows of the liquid.

Note that in all papers mentioned above only the motion of a rigid landslide over a flat slope was considered. In this paper we attempt to simulate surface waves generation by a landslide moving over an uneven slope. We propose a new equation for the motion of a pseudo-rigid landslide and in its derivation take into account the unevenness of the slope, the forces of gravity, buoyancy, friction, and drag. A pseudo-rigid landslide means a body whose surface form changes in accordance with the slope relief where this landslide moves. In this case the horizontal velocity components of all points of the landslide are equal. For a flat slope the obtained equation coincides with the equations presented in [17, 21]. Note that in the numerical simulation of the landslide over a linear slope without friction the authors of [9] joined the slope with an even bottom segment at some depth and, in order to prevent the landslide entering this segment, artificially changed the motion velocity at the end of the slope so that the landslide stopped at a specified position. This artificial sharp braking generated a velocity bend (jump of acceleration) which, in its turn, promoted the appearance of ‘braking waves’ having a considerable amplitude. The consideration of friction leads to a more smooth braking of the landslide and removes such peculiarities from the wave mode.

The simulation of surface waves generated in the motion of a landslide over an uneven bottom was performed within the nonlinear shallow water model subject to the mobility of the bottom. A modified finite difference MacCormack scheme on a fixed uniform grid was used for the calculation [5].

The basic constant characteristics of the wave processes and the parameters depending on the singularities of the form of the underwater slope were determined from the results of numerical experiments. The results of comparison of wave modes over different bottom reliefs are discussed, the dependences of the characteristics of these modes on the geometric and physical parameters of the studied phenomena,

i.e., on the bedding depth of the landslide, its length and thickness, and also the slope geometry and the magnitude of the force of friction are analyzed. It is shown that the pattern of the generated surface waves obtained for the landslide motion over an uneven bottom essentially differs from the case of a flat slope.

1. General statement of the problem

Consider a flat liquid layer bounded by a free surface from above and by a watertight movable bottom from below. It is assumed that the liquid experiences the force of gravity, is incompressible and non-viscous. Let the Cartesian coordinate system Oxz be taken, so that the equation of the free liquid surface at rest has the form $z = 0$ and all characteristics of the liquid depend only on the variables x, t. In order to model the hydrodynamic parameters of the studied phenomena, we use the nonlinear shallow water model whose equations have the following form in the chosen coordinate system:

$$\frac{\partial \mathbf{u}}{\partial t} + \frac{\partial \mathbf{f}}{\partial x} = \mathbf{G} \tag{1.1}$$

where t is the time, $\mathbf{u}$ is the solution vector, $\mathbf{f}$ is the flux vector,

$$\mathbf{u} = \begin{pmatrix} H \\ Hu \end{pmatrix}, \quad \mathbf{f}(\mathbf{u}) = \begin{pmatrix} Hu \\ Hu^2 + gH^2/2 \end{pmatrix}, \quad \mathbf{G} = \begin{pmatrix} 0 \\ gHh_x \end{pmatrix}$$

$u(x,t)$ is the velocity, $H = \eta + h$ is the total depth, $\eta(x,t)$ is the deviation of the free surface from the unperturbed level $z = 0$, the equation

$$z = -h(x,t) = h_{\mathrm{bt}}(x) + h_{\mathrm{sl}}(x,t)$$

determines the form of the movable bottom, $h_{\mathrm{bt}}(x)$ and $h_{\mathrm{sl}}(x,t)$ are the functions determining its fixed and movable parts, respectively, g is the acceleration of gravity.

We assume that a vertical impermeable wall is positioned on the left ($x = 0$) 'coastal' boundary of the water area and the right 'deep-water' boundary is open. The conditions of nonpercolation and free passage are posed on these boundaries, respectively.

It is supposed that at the initial time moment the liquid is in the state of rest and the function $z = h^0_{\mathrm{sl}}(x)$ describing the initial form of the landslide is known:

$$h_{\mathrm{sl}}(x,0) = h^0_{\mathrm{sl}}(x). \tag{1.2}$$

The form and the position of the landslide for $t > 0$ is determined by the law of its motion, this law will be derived in the next section.

The results [2, 3] of the simulation of surface waves generated by a landslide moving over a flat slope give us the ground to assert that the mathematical model presented here provides a sufficiently adequate conception of the studied wave process. In this paper this model is used for the study of surface waves arising in the motion of a landslide over an uneven slope determined by a single-valued function

$$z = h_{\mathrm{bt}}(x). \tag{1.3}$$

The numerical experiments were performed on a uniform calculation grid with the use of a simple and efficient finite difference scheme constructed on the base of the MacCormack scheme of the second order of approximation. The time step was chosen from the stability condition for the finite difference scheme so that the Courant number was equal to 0.9.

2. Law of motion of an underwater landslide

One of the principal factors determining the peculiarities of the wave-formation process caused by the motion of an immersed (underwater) landslide is the motion law associated with this body. In simulating a landslide by a rigid body, such law is specified for a typical point of the body, for example, for its center of mass. The motion laws for landslides proposed in [8, 17, 22, 25] were used by the authors of this paper in their previous investigations when the phenomenon was simulated for the simplest water areas shaped as a 'linear slope'. In this paper we take into account the unevenness of the underwater slope in the derivation of the landslide motion law.

It is supposed that at the initial time moment the landslide has a finite length b and a thickness T and its surface is described by the function

$$z = h_{\mathrm{bt}}(x) + h_{\mathrm{sl}}^0(x) \tag{2.1}$$

where $z = h_{\mathrm{sl}}^0(x)$ is a given nonnegative function with a finite support $\left(x_l^0,\, x_r^0\right)$ of the length b (along the axis Ox) and with the maximal value $T > 0$ at some point of the segment $\left(x_l^0,\, x_r^0\right)$.

For $t > 0$ the landslide can begin its motion over the sloping bottom. Let us describe the simplified method of modelling the landslide process used in this paper and based on the following assumptions:

(1) in the derivation of the landslide motion law, at each time moment this landslide is identified with some material point $\mathbf{x}_c(t)$ having the abscissa $x_c(t)$ and sliding along uneven bottom (1.3) according to the law of motion of a material point along a flat curve, in this case $x_c(0) = x_c^0$, where $x_c^0 \in \left(x_l^0,\, x_r^0\right)$;

(2) the position of the landslide is exclusively determined by the value of the abscissa $x_c(t)$ of the selected point $\mathbf{x}_c(t)$, and its surface is described for $t > 0$ by the function

$$z = h_{\mathrm{bt}}(x) + h_{\mathrm{sl}}(x,t) \tag{2.2}$$

where $h_{\mathrm{sl}}(x,t) = h_{\mathrm{sl}}^0(x + x_c^0 - x_c(t))$.

Thus, at the time moment t the landslide is positioned on the slope between the points with the abscissas

$$x_l(t) = x_l^0 - x_c^0 + x_c(t), \qquad x_r(t) = x_r^0 - x_c^0 + x_c(t) = x_l(t) + b \tag{2.3}$$

and in the course of motion its length (along the horizontal axis Ox) remains invariable. Note also that in the motion of the landslide its surface is deformed according to the raggedness of the bottom, however, the volume V of the landslide and its mass $M = \rho_{\mathrm{sl}} V$ remain invariable. Here ρ_{sl} is the density of the material of the landslide.

Describe the landslide motion law, or more exactly, indicate the method of calculation of the function $x = x_c(t)$, because just this function participates in the definition of surface (2.2) of the moving landslide.

Let s be the arc length of curve (1.3) measured from its beginning. By assumption, (1.3) is a single-value function of the variable x and hence there is one-to-one correspondence between the variables x and s, which is given by the equality

$$s(x) = \int_0^x \sqrt{1 + \left[\, h'_{\rm bt}(\xi) \,\right]^2}\, \mathrm{d}\xi. \tag{2.4}$$

Suppose the selected point $\mathbf{x}_c(0)$ corresponds to the parameter $s = S_0$ and the moving point $\mathbf{x}_c(t)$ with the abscissa $x_c(t)$ corresponds to the parameter $s = S(t)$. Then the law of motion $s = S(t)$ of the initially resting material point $\mathbf{x}_c(t)$ along curve (1.3) has the following form:

$$m\ddot{S}(t) = F_\tau(t), \qquad S(0) = S_0, \qquad \dot{S}(0) = 0 \tag{2.5}$$

where $\ddot{S} = \mathrm{d}^2S/\mathrm{d}t^2$, $\dot{S} = \mathrm{d}S/\mathrm{d}t$, m is a value having the dimensionality of mass, $F_\tau(t)$ is the tangent component of the force acting onto the moving point $\mathbf{x}_c(t)$ at the time moment t.

For the value of m we take the sum of the mass M of the landslide and the associated water mass $C_w\rho_w V$, i.e.,

$$m = M + C_w\rho_w V = (\rho_{\rm sl} + C_w\rho_w)V \tag{2.6}$$

where ρ_w is the water density taken equal to one in the calculations, C_w is the coefficient of the associated mass.

Now clarify the notion of the force F_τ entering equation (2.5) and acting on the material point $\mathbf{x}_c(t)$. The force of gravity and the buoyancy force act on each element of the length $\mathrm{d}x$ of the landslide in the vertical direction. At an arbitrary point $x \in (x_l(t),\, x_r(t))$, the component of these two opposite forces which is tangent to curve (1.3) can be calculated by the formula

$$(\rho_{\rm sl} - \rho_w)\, h_{\rm sl}(x,t) W g \sin\theta(x)\, \mathrm{d}x \tag{2.7}$$

where W is the landslide width perpendicular to the plane xOz, $\theta(x)$ is the local slope angle of the bottom, in this case

$$\theta(x) = -\arctan h'_{\rm bt}(x), \qquad \sin\theta(x) = -\frac{h'_{\rm bt}(x)}{\sqrt{1 + \left[\, h'_{\rm bt}(x) \,\right]^2}}.$$

Thus, the total effect of the gravity and buoyancy forces on the landslide of a finite size is replaced by the force

$$(\rho_{\rm sl} - \rho_w) W g \int_{x_l(t)}^{x_r(t)} h_{\rm sl}(x,t) \sin\theta(x)\, \mathrm{d}x \tag{2.8}$$

acting in the tangent direction on the material point $\mathbf{x}_c(t)$ moving along curve (1.3).

Force (2.8) accelerates the landslide, and deceleration is caused by the drag and friction of the landslide against the bottom. The tangent component of the drag opposite to the motion of the landslide is proportional to the area TW of its greatest cross-section and is equal to

$$-\frac{1}{2}C_d\rho_w TW(\dot{S})^2 \tag{2.9}$$

where $\dot{S}$ is the velocity of the point $\mathbf{x}_0(t)$ along curve (1.3), C_d is the drag coefficient. Note that drag (2.9) is passive, i.e., this force vanishes in the absence of motion.

Another force decelerating the motion of the landslide is the force of friction directed along the tangent to curve (1.3) opposite to the motion of the landslide. This force is passive too, because in the absence of motion it cannot change the position of the landslide and its effect on the position of the landslide becomes apparent only in its motion (for $\dot{S} \neq 0$).

First we consider an element of length dx of the landslide. We determine the force of friction for it based on the normal reaction $N(x,t)$ from the bottom to the selected element:

$$F_f(x,t) = -C_f N(x,t) \tag{2.10}$$

where C_f is the dynamic coefficient of friction (the sliding friction coefficient). In our simplified model of the landslide process we assume that the numerical value of the coefficient C_f coincides with the value of the sliding friction coefficient at rest and is determined by the friction angle θ_*, i.e., the threshold value of the angle is such that the excess of this angle initiates sliding of the landslide over the flat slope. This angle of friction is also used for curvilinear slopes. The assumptions presented above imply the following formula for the determination of the friction coefficient:

$$C_f = \tan\theta_*.$$

The normal reaction $N(x,t)$ acting on the element dx of the landslide is determined as the sum of the normal component of the force of gravity and the centrifugal force:

$$N(x,t) = (\rho_{\mathrm{sl}} - \rho_w)\, h_{\mathrm{sl}}(x,t) W g \cos\theta(x)\,\mathrm{d}x + (\rho_{\mathrm{sl}} - \rho_w)\, h_{\mathrm{sl}}(x,t) W K(x) \left(\dot{S}(t)\right)^2 \mathrm{d}x \tag{2.11}$$

where $K(x)$ is the bottom curvature of a fixed sign:

$$K(x) = h''_{\mathrm{bt}}(x) \left(\sqrt{1 + \left[\, h'_{\mathrm{bt}}(x) \,\right]^2} \right)^{-3}.$$

The curvature equals zero for a flat slope, therefore, for this case expression (2.11) does not contain the second summand. It is also seen from formulas (2.10), (2.11) that, in comparison with a flat slope, the unevenness of the bottom causes some decrease in the force of friction (in its absolute value) on the upward convex

segments of the bottom ($h''_{\rm bt}(x) < 0$) and vice versa, some increase in the downward convex segments ($h''_{\rm bt}(x) > 0$).

Taking into account expression (2.11), we get that the following force of friction acts on the moving landslide (this force is applied at the point $\mathbf{x}_c(t)$ and is tangent to curve (1.3) at this point):

$$F_f(t) = -C_f\,(\rho_{\rm sl} - \rho_w)\,W \int\limits_{x_l(t)}^{x_r(t)} h_{\rm sl}(x,t)\Big[g\cos\theta(x) + K(x)\left(\dot S(t)\right)^2\Big]\,{\rm d}x. \qquad (2.12)$$

The resultant force of (2.8), (2.9), (2.12) is accepted as F_τ entering formula (2.5). Thus, taking into account the above assumptions, problem (2.5) is written in the following form:

$$(\rho_{\rm sl} + C_w\rho_w)\,V\ddot S = (\rho_{\rm sl} - \rho_w)\,W g I_1 - W\left[(\rho_{\rm sl} - \rho_w)\,I_2 + \frac{1}{2}C_d\rho_w T\right](\dot S)^2 \qquad (2.13)$$

$$S(0) = S_0, \qquad \dot S(0) = 0 \qquad (2.14)$$

where

$$I_1(t) = \int\limits_{x_l(t)}^{x_r(t)} h_{\rm sl}(x,t)\Big[\sin\theta(x) - C_f\cos\theta(x)\Big]\,{\rm d}x, \qquad I_2(t) = C_f\int\limits_{x_l(t)}^{x_r(t)} h_{\rm sl}(x,t)K(x)\,{\rm d}x$$

and the required value $x_c(t)$ is related to the solution $S(t)$ to problem (2.13), (2.14) by relation (2.4):

$$S(t) = \int\limits_0^{x_c(t)} \sqrt{1 + \left[\,h'_{\rm bt}(\xi)\,\right]^2}\,{\rm d}\xi.$$

Note that equation (2.13) is valid only for a moving landslide. Since the landslide is at rest at the initial moment, we can use this equation for $t > 0$ only if the landslide actually starts to move. The form of equation (2.13) implies that the sufficient condition for the possibility of the landslide to move at the initial time moment is the positivity of the integral I_1 at $t = 0$:

$$I_1 = \int\limits_{x_l^0}^{x_r^0} h_{\rm sl}^0(x)\Big[\sin\theta(x) - C_f\cos\theta(x)\Big]\,{\rm d}x > 0.$$

Since equation (2.13) is nonlinear, we have to use numerical methods for its solution. To do that, it is expedient to rewrite problem (2.13), (2.14) as a Cauchy problem for a system of first-order ordinary differential equations:

$$(\gamma + C_w)\,\frac{V}{W}\,\dot v = (\gamma - 1)\,g I_1 - \left[(\gamma - 1)\,I_2 + \frac{C_d}{2}T\right]v^2, \qquad v(0) = 0 \qquad (2.15)$$

$$\dot{S} = v, \qquad S(0) = S_0 \tag{2.16}$$

where $\gamma = \rho_{\text{sl}}/\rho_w$ denotes the ratio of the density of the landslide material to the water density, $\gamma > 1$. The solution to this problem is sought up to the stopping moment of the landslide, i.e., up to the time moment when the landslide velocity v first turns to zero (with a given accuracy).

3. Model water areas and model landslide

3.1. Model water areas

For the first attempts to study the effect of the bottom unevenness on the surface waves generated by the motion of an underwater landslide we have chosen two model reliefs. The simplest model relief is a linear slope with the inclination angle $\theta = 2^\circ$ from the depth of 20 m on the left boundary to the depth of 1400 m passing to the zone of a constant depth up to the right boundary $x = 70000$ m:

$$h_{\text{bt}}(x) = \begin{cases} -20 - x\tan 2^\circ, & 0 \leqslant x \leqslant 1380\cot 2^\circ \\ -1400, & 1380\cot 2^\circ \leqslant x \leqslant 70000. \end{cases}$$

The second (curvilinear) relief with a nonzero curvature was obtained with the help of an analytic smooth monotone decreasing function:

$$h_{bt}(x) = \frac{h_+ + h_-}{2} + \frac{h_+ - h_-}{2}\tanh\left[c(x-\xi)\right]$$

where h_+ is the bottom depth at the right infinitely distant point, h_- is the depth at the left infinitely distant point, $c = 2\tan\theta_0/(h_- - h_+)$, θ_0 is the maximal slope angle of the relief, $\xi = (1/2c)\ln(h_0 - h_+)/(h_- - h_0)$ is the point of bending, h_0 is the depth at the point $x = 0$. We used the following values of the parameters in the calculations: $h_+ = -1400$ m, $h_- = -15$ m, $\theta_0 = 6^\circ$, $h_0 = -20$ m. The length of the domain was 70000 m. Further we call this relief 'curvilinear'.

We used four virtual mareographs for recording the results, they were positioned on the shore ($x = 0$ m, mareograph A), over the upper part of the slope ($x = 10000$ m, mareograph B), near the end of the slope ($x = 30000$ m, mareograph C), and in the deep-water zone ($x = 60000$ m, mareograph D). The total number of the calculation grid nodes used in the numerical experiments was 1401.

3.2. Model landslide

The form of a rigid body for the model landslide used by the authors in the study was defined by the formula similar to that proposed in [16]:

$$h_{sl}(x,t) = T\frac{\left[1+\tanh\left(2(x-x_1(t))/p\right)\right]\left[1-\tanh\left(2(x-x_2(t))/p\right)\right]}{\left[1+\tanh(1)\right]\left[1-\tanh(-1)\right]}$$

where $x_1(t) = x_c(t) - p/2,\ x_2(t) = x_c(t) + p/2,\ x_c(t)$ is the coordinate of the center of mass of the landslide on the axis Ox.

The maximal depth T of the landslide was taken equal to 25 m, the parameter p corresponding to the length of the landslide was 2500 m. Since in the derivation of the motion law we assumed that the length of the landslide is finite, the support of the landslide was determined by 10 % of the maximal thickness and so its length b was approximately equal to 5000 m. At the initial time moment the center of mass of the landslide was at the point corresponding to the depth of 500 m. These values, along with the values of the constants in this law of motion ($\gamma = 1.5$, $C_w = 1$, $C_d = 1$, $\theta_* = 1^\circ$) are used in numerical experiments by default if we do not specify otherwise.

4. Numerical experiments

4.1. General characteristics of generated wave modes

Considering the peculiarities of the landslide mechanism of wave formation related to the complication of the bottom relief, we have to note that the nonlinearly varying bottom relief, first, influences the wave transformation in its spread and, second, participates in the formation of the landslide motion law depending on the local slope angle $\theta(x)$.

The plots of time variations of the velocities and acceleration of the centers of mass of landslides (Fig. 2) illustrate the laws of motion of landslides moving under the effect of the gravity, buoyancy, friction, and drag forces. Here and further the velocity was calculated directly from the equations of the landslide motion, and the acceleration was calculated by central finite differences and further averaging by the five-points moving average method.

As can be seen from the plots, at the initial time moment the body begins to move with some acceleration decreasing in time. When the body moves over the linear slope, before the transition to the deceleration mode acceleration slowly tends to its zero value, and over curvilinear zones the passage to the deceleration mode takes place much faster. As was already noted above (in the derivation of the motion law), the force of friction decreases in the zone of acceleration over an upward convex part of the slope, which promotes acceleration, whereas the contribution of the force of friction increases near the end of the slope over the downward convex part and hence intensifies the braking process.

It is worth noting that if the linear slope were infinite, the motion velocity of the landslide under the effect of the resultant external force would asymptotically tend to some finite limit, whose value is determined by the parameters of the slope and the landslide.

When the landslide enters the zone of small slope angles, the process of deceleration begins and the highest rate of this process is observed at the initial stage of deceleration, then it is gradually decreases to the complete stop of the landslide. This stop occurs sharply (with a jump of acceleration) under a nonzero contribution

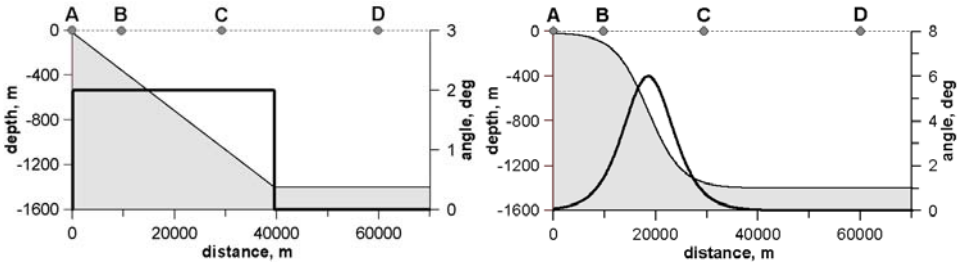

Figure 1. Plots of the bottom relief characteristics of model water areas used in numerical experiments: depth distribution (shading, left axes) and slope angles (solid lines, right-hand axes); the linear slope (left) and the curvilinear slope (right). The position of virtual mareographs are marked at the top.

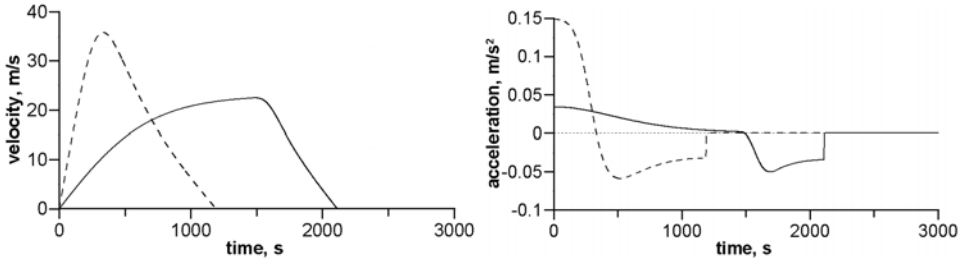

Figure 2. Plots of velocity and acceleration variation in landslides moving over different model slopes: solid line – linear slope; dotted line – curvilinear slope.

of the force of friction, but if the force of friction is not taken into account, then, as will be shown further, a completely smooth braking is observed.

The analysis of the graphs also shows that for the considered bottom reliefs the maximal velocity is attained by a landslide moving over the 'curvilinear' slope, and in this case the duration of its motion until a complete stop is shorter, the velocity changes faster at the acceleration stage, and at the deceleration stage it is approximately the same. However, the duration of braking over the curvilinear slope is greater, whereas over the linear slope the stage of acceleration lasts much longer.

The patterns of free surface dynamics corresponding to these parameters are presented in the series of figures (Figs. 3 and 4) and will be discussed further. In these figures, the dotted lines mark the positions of virtual mareographs, the vertical axis indicates time in seconds, the horizontal axis indicates the distance from the wall in meters.

It is the easiest to consider the basic characteristics of the landslide mechanism of wave formation by the example of the process in a water area with the simplest linear bottom relief. As is seen from Fig. 3, two waves appear when the landslide starts, one of them, i.e., the wave of elevation, is pushed by the landslide toward the deeper area. Its amplitude is almost constant, whereas its length is increased under the acceleration of the body: its front goes into the open sea approximately at the velocity of small perturbations $\sqrt{g(h(x))}$, and its back goes before the landslide (which acts as the wave generator) at a sub-critical velocity, i.e., the wave is permanently 'fed' by the accelerated body. When the main phase of acceleration ends,

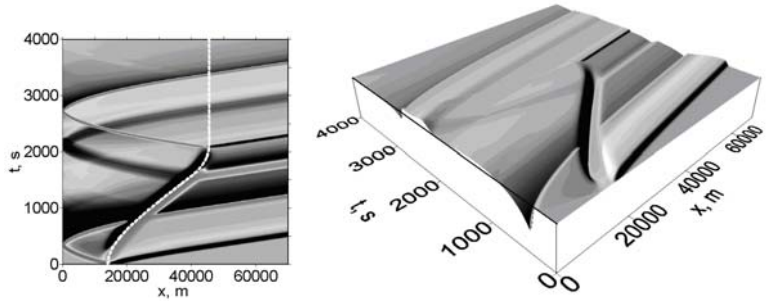

Figure 3. Path of the center of mass of a landslide moving over a linear slope (left, white dotted line) and the corresponding free surface dynamics.

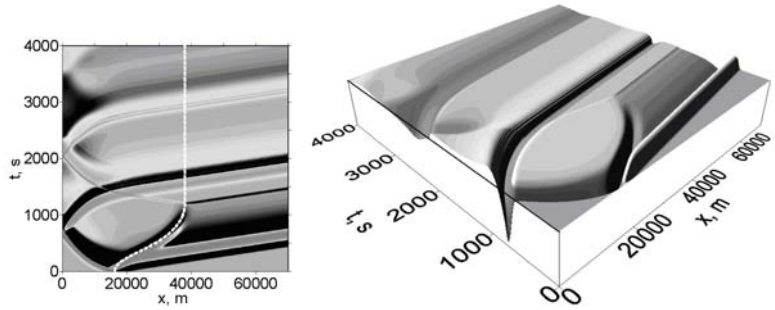

Figure 4. Path of the center of mass of a landslide moving over a curvilinear slope (left, white dotted line) and the corresponding free surface dynamics.

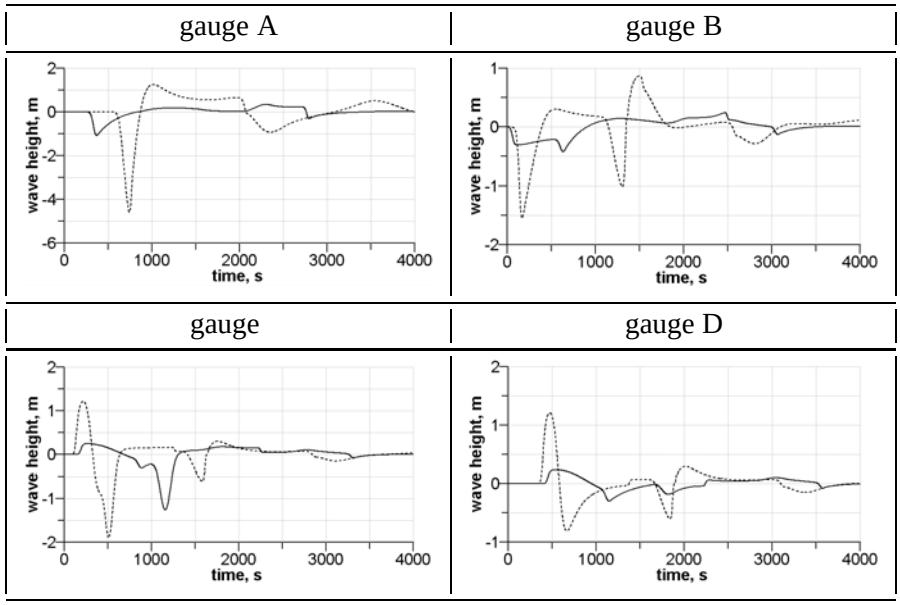

Figure 5. Comparison of the mareograms: solid line – linear slope; dotted line – curvilinear slope.

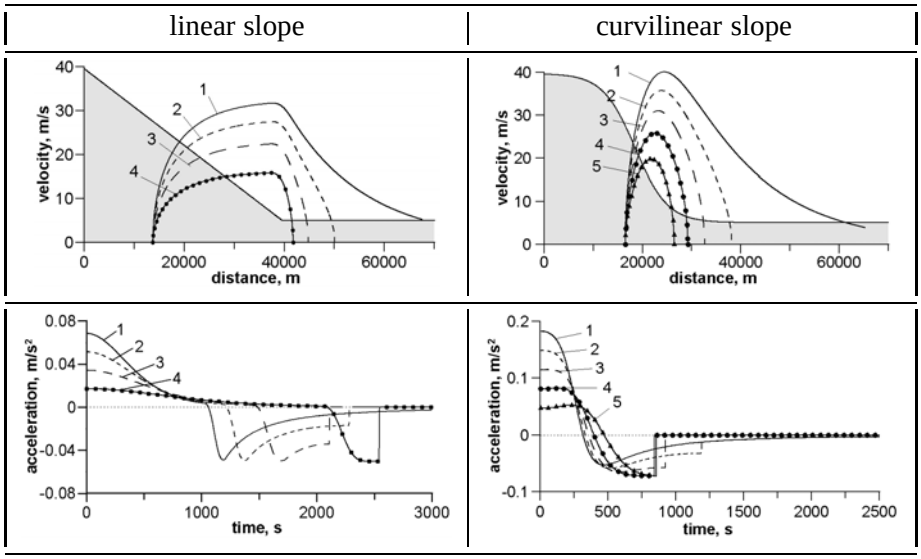

Figure 6. Characteristics of the law of motion of a landslide for different friction angles θ_*. For the linear slope: (1) – 0.0°, (2) – 0.5°, (3) – 1.0°, (4) – 1.5°. For the curvilinear slope: (1) – 0.0°, (2) – 1.0°, (3) – 2.0°, (4) – 3.0°, (5) – 4.0°.

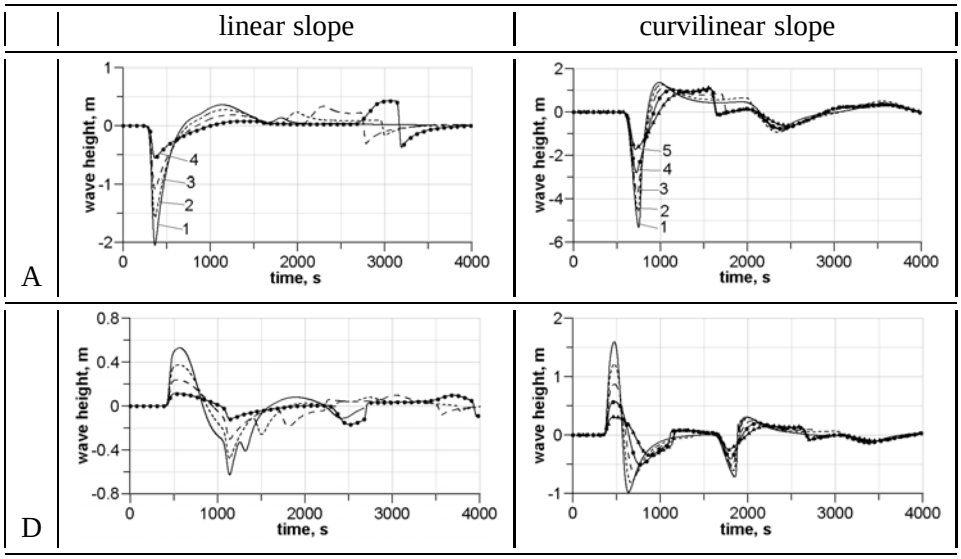

Figure 7. Mareograms calculated by mareographs A and D for different friction angles θ_*. For the linear slope: (1) – 0.0°, (2) – 0.5°, (3) – 1.0°, (4) – 1.5°. For the curvilinear slope: (1) – 0.0°, (2) – 1.0°, (3) – 2.0°, (4) – 3.0°, (5) – 4.0°.

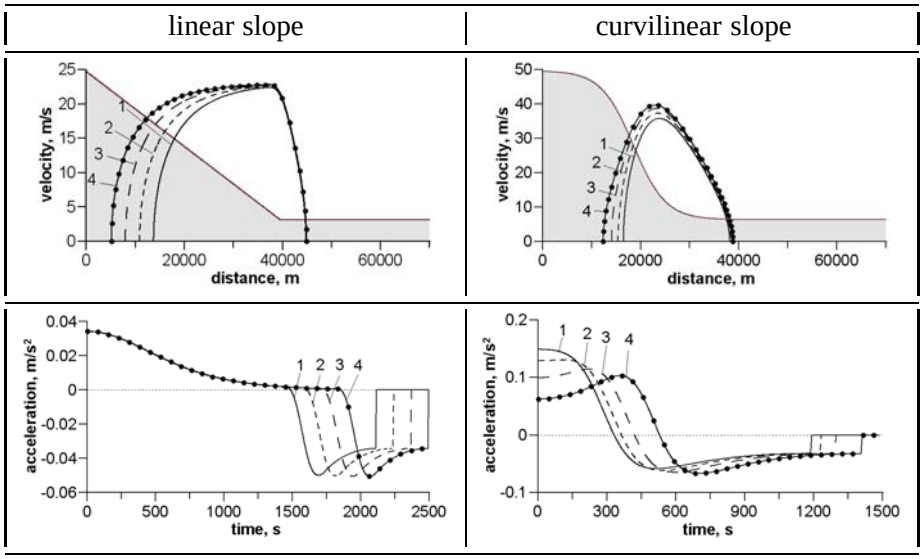

Figure 8. Characteristics of the law of motion of a landslide for different depths of the initial position of the mass center d_c: (1) – 500 m, (2) – 400 m, (3) – 300 m, (4) – 200 m.

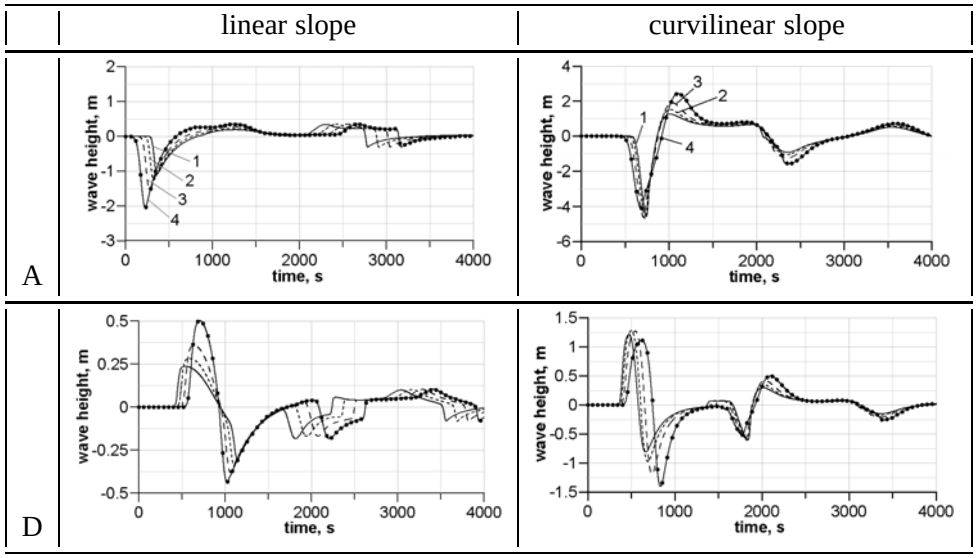

Figure 9. Mareograms calculated for different depths of the initial depths d_c: (1) – 500 m, (2) – 400 m, (3) – 300 m, (4) – 200 m.

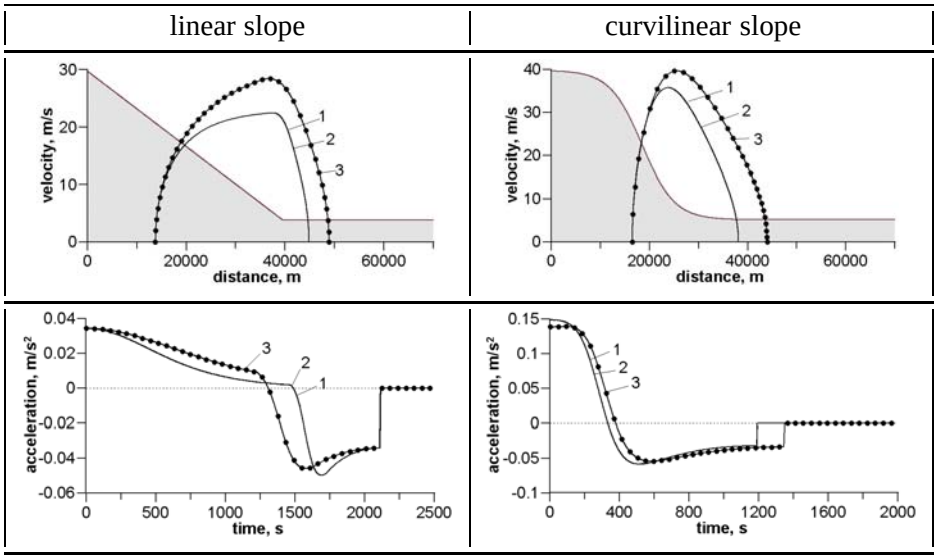

Figure 10. Characteristics of the law of motion of a landslide for different landslide sizes: (1) – 'standard' landslide, (2) – landslide with double thickness, (3) – landslide with double length.

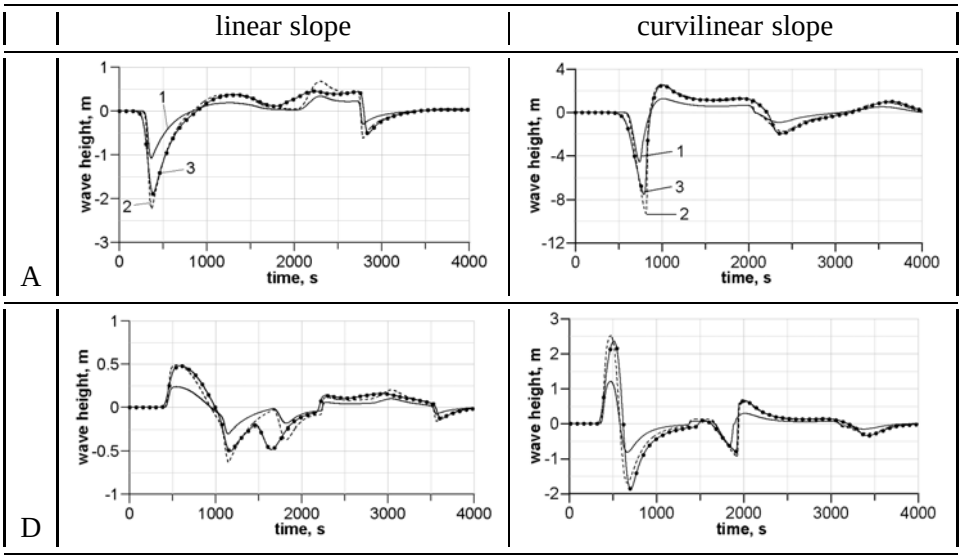

Figure 11. Mareograms calculated for different landslide sizes: (1) – 'standard' landslide, (2) – landslide with double thickness, (3) – landslide with double length.

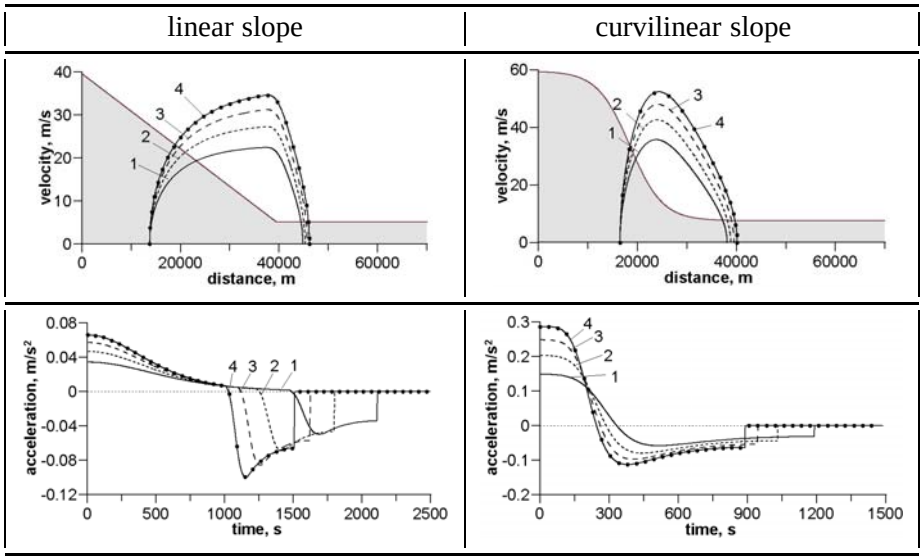

Figure 12. Characteristics of the law of motion of a landslide for different density ratios γ: (1) – $\gamma = 1.5$, (2) – $\gamma = 1.75$, (3) – $\gamma = 2.0$, (4) – $\gamma = 2.25$.

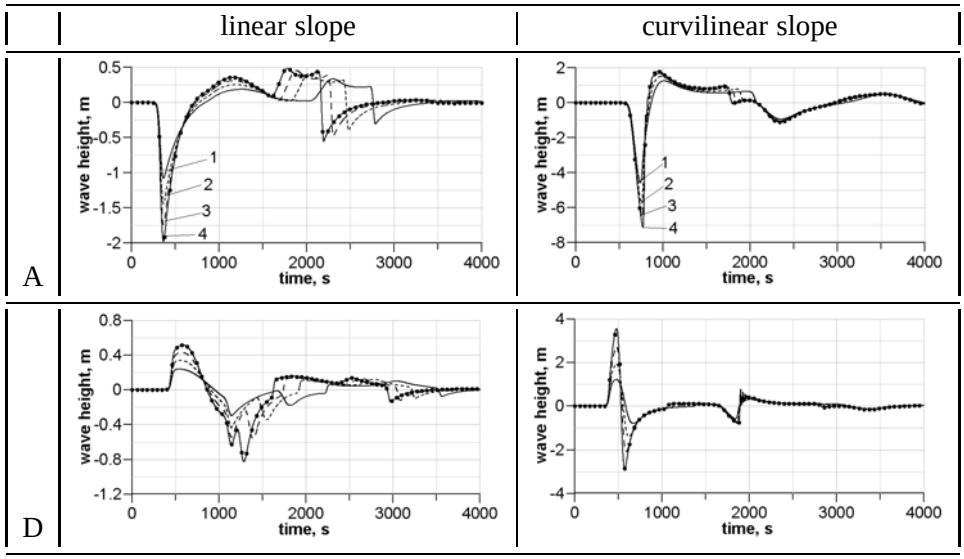

Figure 13. Mareograms calculated for different density ratios γ: (1) – $\gamma = 1.5$, (2) – $\gamma = 1.75$, (3) – $\gamma = 2.0$, (4) – $\gamma = 2.25$.

this wave separates from the body and goes off through the right open boundary. As the landslide moves almost uniformly down the slope, a small lowering wave is generated before it and a wave of elevation is generated after it.

The second wave arising at the start (lowering wave) is split into two parts, and one of these parts goes to the shore. During the motion up the slope, its amplitude slightly increases. Another lowering wave moves directly over the landslide toward the open sea until the landslide stops. The amplitude of this wave increases at the stage of the acceleration of the landslide, but this effect is partly compensated by the drift of the landslide into the zone of greater depths.

When the landslide moves down the sloping bottom at an almost constant velocity (beginning with the time moment of approximately 800 s) and also in its deceleration in the area of a constant depth, the amplitude of the lowering wave above it monotonically decreases and for small velocities the wave becomes practically indistinguishable.

Reverting to the 'coastal' lowering wave, note that this wave is reflected from the wall positioned on the left boundary and then overtakes the landslide and interacts with the wave accompanying it (in this case the 'tail' of the negative wave moving down the slope takes positive values and generates an elevation wave on the left wall). This also occurs approximately 800 seconds after the beginning of the process. At the next stages, the wave reflected from the wall continues its way toward deep water and leaves through the open boundary.

Two long waves, opposite in their sign and direction of propagation are formed in the braking of the landslide. These waves have small amplitudes, sufficiently gentle fronts, and steep backs (as the consequence of an abrupt stop). The negative wave goes into the open sea, the positive one goes to the shore (after its reflection and backward motion over the sloping bottom, a lowering wave appears on the wall).

The further comparison of the results obtained for different model reliefs is performed with the use of mareograms calculated at different mareograph points. The general idea can be obtained by comparing mareograms registered by the same mareographs for different reliefs (Fig. 5). In this case we should take into account the differences in the formation of landslide velocities on different reliefs (Fig. 2). The considerable predominance (by almost four times) of the amplitude of the negative wave near the shore calculated over the curvilinear slope is due to the significant predominance of acceleration. The difference in the depth distribution in the coastal zone is manifested in some delay of the 'wave on the curvilinear slope' compared to the 'wave on the linear slope'.

In the case of the curvilinear slope, the mareograph A explicitly shows the wave with a positive amplitude caused by the confluence of the group of waves consisting of the elevation waves generated after the lowering waves going to the deeper zone (the wave over the landslide and the wave reflected from the wall) and also the elevation wave generated by the stop of the landslide.

In the case of the linear slope the stop of the landslide occurs considerably later and thus the positive wave generated by it does not merge with the first two.

The mareograms calculated at the point with the coordinate $x = 10000$ m allow

us to see separately all important components of the wave mode generated by the landslide mechanism in the coastal zone. The predominance of the depths of the linear slope near the shore is manifested in the fact that the waves reflected from the shore come to this point earlier. The positive impulse following the reflected lowering wave over the curvilinear slope is the result of the above-mentioned confluence of the set of positive traces of the lowering waves and the wave generated by the stop of the landslide. This structure is not formed at this point in the case of the linear slope.

The mareograph *C* is the only instrument registering the transition of the landslide and the related wave effects. One can easily discern in its readings the positive wave pushed by the landslide and two lowering waves following it. On the linear slope the first of these waves is the one reflected from the shore and the second one (with the greater amplitude) is the lowering wave going directly over the body. On the curvilinear slope these two waves come to the mareograph *C* in a reverse order. The similar reverse order of the negative waves takes place at the mareograph *D* except for the fact that these lowering waves are the wave reflected from the wall and the wave generated in the braking of the body.

4.2. Dependence on the value of the friction angle

In order to study the effect of the friction angle θ_* on the motion of the body and on the characteristics of the waves generated in this process, we considered the following values of θ_*: for the linear slope they were 0.0, 0.5, 1.0, and 1.5 degrees (for the values $\theta_* \geqslant 2^\circ$ the landslide does not move), for the curvilinear slope they were 0.0, 1.0, 2.0, 3.0, and 4.0 (here for $\theta_* \geqslant 5^\circ$ there is no motion of the landslide).

Below (Fig. 6) we present the graphs of the variation of the velocity and acceleration of the center of mass of the body. The representation of the velocity as a function of the spatial variable (the function of the position of the landslide center of mass in space) allows us to estimate the effect of the relief variation on the motion of the landslide. At the same time, the representation of velocities and accelerations as the functions of time allows us to compare the moments of change of the body motion character (in particular, the moments of stop) for different parameters of the problem.

Analysis of the graphs shows that the distance passed by the landslide and its velocity in the course of motion decrease with the growth of friction. The pattern for acceleration is slightly different: positive acceleration also demonstrates a clear inverse dependence on the angle of friction, but the maximal rate of braking on the linear slope practically does not depend on the angle of friction. On the curvilinear slope, the maximal (in absolute value) negative acceleration slightly increases with the growth of the angle of friction. The time of stop of the landslide demonstrates a non-monotone behaviour on both reliefs: as the friction grows, the total time of motion first decreases and then increases. We may also note that on the curvilinear slope for a large angle of friction the acceleration first slightly increases and only after that begins decreasing.

As was already said in the description of the general characteristics of the wave modes generated by an underwater landslide, the first lowering wave registered near the wall is generated at the start of the body motion and then goes toward the shallow water, i.e., in the direction inverse to the motion of the landslide. Its amplitude depends on the initial acceleration, which explains such difference in the registered negative values. The first positive wave registered near the shore is formed when the negative waves (the wave moving above the landslide and the one reflected from the shore, which is generated at the start of the body motion) move along the slope toward deep water. This positive wave is explicitly seen on the linear slope and its amplitude inversely depends on the value of the friction angle (see Fig. 7). The second positive wave appears at the braking of the body and breaks at the moment when the landslide finally stops. The amplitude of this wave is directly proportional to the absolute value of the acceleration just before the stop, therefore, it is the maximum for the case of the greatest angle of friction of the linear slope.

On the curvilinear slope the process of braking develops faster, therefore, both positive waves practically merge, especially for large angles of friction. Here we have the effect that braking occurs at different depths: for large θ_* the depth of the beginning of braking is smaller, which slightly increases the amplitude of the generated wave. As the result, it occurs that the maximal positive amplitude is approximately the same for all considered values of the angle of friction, although for greater values of θ_* this amplitude comes to the shore later, and the length of the corresponding wave is smaller.

Under the variation of the friction force parameters, the waves going toward deep water and spreading over that area experience similar changes.

4.3. Dependence on initial depth

In order to study the influence of the initial depth on the wave formation characteristics, we considered the following different values of initial depth d: 500, 400, 300, and 200 m.

As was to be expected, the character of motion of the landslide on the linear slope presents no differences with respect to the initial depth. Naturally, only the time of arrival of the body to the point of the depth break and the time of deceleration of the body on the even bottom are different. Due to the equality of the velocities by the moment of this deceleration, the point of stop of the body is the same in all the cases. On the curvilinear slope the situation is slightly different: the smaller depths are observed here in zones with smaller bottom slope angles. Therefore, the initial acceleration of landslides starting from smaller depths are lower as well. However, as such landslide moves and comes to the zone with the maximal slope angle, the acceleration of the ‘shallow water’ landslide grows and almost reaches the values that the ‘deep water’ landslides reach mush faster. The maximal values of the velocities increase, as the depth decreases, and the points of stop of landslides differ insignificantly for any initial depth.

The dependence of the motion laws of underwater landslides on the initial

depth of the center of mass becomes apparent in the generated wave modes, so that whereas the amplitude of the first negative wave going into the zone of smaller amplitudes on the linear slope monotonically increases with the decrease of the initial depth of the center of mass, on the curvilinear slope the decrease in the initial depth leads to an insignificant decrease in the amplitude of the wave trough. The amplitudes of the first positive waves near the 'shore' change practically identically over different slopes under the decrease of the depth: the smaller the depth, the greater the amplitude. However, one can notice that on the linear slope the time of the arrival of the first positive wave decreases with decreasing depth, whereas on the curvilinear slope the dependence is reverse. The amplitudes of the second waves generated in the braking of the body are approximately the same for all initial depths, which is in good accordance with the equality of the velocities and accelerations under braking and the final stop.

The mareograph D registers a similar pattern as a whole. On the linear slope the positive wave pushed by the body and the negative one following it (reflected from the shore) indicate a sufficiently strong direct dependence on the depth, and the next lowering wave appearing at the braking of the body in all the cases is the same, as well as the forthcoming 'tail', which is the effect of the positive 'wave of braking' reflected from the left wall. In contrast to the linear slope, on the curvilinear slope the first positive wave pushed by the landslide and the second negative wave coming after the reflection from the wall slightly decrease with increasing depth. On the contrary, the second positive and the first negative 'waves of braking' demonstrate direct dependence on the initial depth.

4.4. Dependence on the size of the body

In order to study the dependence of the parameters of the wave mode generated by the landslide on its spatial characteristics (length and thickness), we performed the calculations where these characteristics were doubled with respect to the standard values. Thus, we considered the cases $b = 5000$ m, $T = 25$ m (standard); $b = 5000$ m, $T = 50$ m (double thickness); $b = 10000$ m, $T = 25$ m (double length).

As is seen from the graphs in Fig. 9, the law of motion of the landslide does not vary under the change of its thickness (this directly follows from the formula of the law of motion), but the increase in the landslide length is expressed differently on different slopes. On the one hand, this is caused by the specifics of the entrance of the parameter of length into the formula of the motion law and, on the other hand, by the fact that with the increasing length the landslide body covers additional sections of the slope where the inclination angle may vary. For the curvilinear landslide this effect becomes apparent from the very beginning of the motion, but for the linear slope this occurs when the landslide goes from the sloping area to the bottom of a constant depth. Thus, on the linear slope the initial acceleration of the landslide does not depend on its length and the maximal absolute value of its negative magnitude at braking on an even area is slightly less, because as the length of the landslide grows, its left side remains on the sloping area for a longer time. On the curvilinear slope,

the initial acceleration decreases with the increasing length, and braking before the complete stop is slower. In total, the velocity for a longer landslide is higher.

Concerning the generated waves (Fig. 11), the double increase of the sizes results identically in an almost similar increase in the amplitudes of the positive and negative waves. The effect of the double increase of the wave amplitudes under the double increase in sizes holds for the curvilinear slope as well. In some fragments of the mareograms the effect of the double increase of the landslide thickness is expressed stronger.

4.5. Dependence on density characteristics

The relationship between the parameters of the surrounding liquid and the landslide, the laws of its motion, and the characteristics of the wave modes generated by that motion seems the simplest. The independent variable of the required dependence is the ratio of the densities $\gamma = \rho_{sl}/\rho_w$. In the calculations this parameter took four values: 1.5, 1.75, 2.0, 2.25.

For each of the model water areas, if the ratio of the densities γ grows, the landslide velocity monotonically grows, the maximal absolute values of the speeding-up and braking also grow, the durations of motion are in the inverse dependence, and the coordinate of the final stop remains practically unchanged (Fig. 12).

The monotonicity of the dependence of the landslide motion characteristics on the ratio of densities is translated onto the characteristics of the wave mode registered by the three virtual mareographs (Fig. 13). The amplitudes of the positive and negative waves monotonically grow with the growth of the parameter γ.

5. Conclusion

In the study of the landslide mechanism of surface waves formation, we made an attempt to proceed from the consideration of the simplest linear slopes to curvilinear ones. This attempt allowed us to obtain a series of new results. The most important of these results is the derivation of the motion law for an underwater pseudo-rigid landslide. This law takes into account the curvature of the slope where the landslide moves under the effect of the forces of gravity, buoyancy, friction, and drag.

The numerical experiments performed with the use of the new motion law demonstrated the peculiarities caused by variations of landslide sizes, of initial depth, of density characteristics and friction coefficients on different reliefs. It was shown that the peculiarities of the wave modes generated by an underwater landslide are mainly determined by the peculiarities of the landslide acceleration and by the dependence of this acceleration on the parameters of the phenomenon mentioned above.

References

1. L. B. Chubarov, S. V. Eletskii, Z. I. Fedotova, and G. S. Khakimzyanov, Simulation of surface waves generation by an underwater landslide. *Russ. J. Numer. Anal. Math. Modelling* (2005) **20**, No. 5, 425–437.
2. L. B. Chubarov, Z. I. Fedotova, and S. V. Eletskii, Numerical modelling of generation of surface water waves by motion of the drowned soil. In: *Proc. of the Int. Conf. on Comp. Math. ICCM-2004. Part II*. Pub. ICMMG SB RAS, Novosibirsk, 2004, pp. 753–758 (in Russian).
3. S. V. Eletskij, Yu. B. Maiorov, V. V. Maksimov, I. S. Nudner, Z. I. Fedotova, M. G. Khazhoyan, G. S. Khakimzyanov, and L. B. Chubarov, Simulation of surface waves generation by a moving part of the bottom down the coastal slope. *Comp. Tech.* (2004) **9**, Special issue, Part 2, 194–206.
4. F. Enet and S. T. Grilli, Experimental study of tsunami generation by three-dimensional rigid underwater landslides. *J. Waterway Port Coastal and Ocean Engrg.* (2007) **133**, No. 6, 442–454.
5. Z. I. Fedotova, On application of the MacCormack difference scheme for problems of long-wave hydrodynamics. *Comp. Tech.* (2006) **11**, Special issue, Part 2, 53–63.
6. Z. I. Fedotova, L. B. Chubarov, and Yu. I. Shokin, Simulation of surface waves induced by landslides. *Int. J. Fluid Mech. Res.* (2006) **33**, No. 1, 2–14.
7. I. A. Garagash and L. I. Lobkovskij, Geometric estimation of landslide processes and its monitoring on slope of the Black Sea in view of realization of the 'Blue flow' project. In: *Proc. Sixth Int. Sci. Tech. Conf. 'Up-to-date Methods and Tools of Oceanological Investigations'*. Moscow, 2000, pp. 5–15.
8. S. T. Grilli and P. Watts, Modelling of waves generated by moving submerged body. Applications to underwater landslide. *Engrg. Anal. Bound. Elem.* (1999) **23**, 645–656.
9. S. T. Grilli and P. Watts, Tsunami generation by submarine mass failure. I: Modelling, experimental validation, and sensitivity analyses. *J. Waterway Port Coastal and Ocean Engrg.* (2005) **131**, No. 6, 283–297.
10. C. Harbitz and G. Pedersen, Model theory and analytical solutions for large water waves due to landslides. *Preprint Series*, Dept. of Math., Univ. of Oslo, 1992, No. 4.
11. P. Heinrich, A. Piatanesi, and H. Hebert, Numerical modelling of tsunami generation and propagation from submarine slumps: the 1998 Papua New Guinea event. *Geophys. J. Int.* (2001) **145**, 97–111.
12. P. Heinrich, F. Schindele, S. Guibourg, and P. Ihmle, Modelling of the February 1996 Peruvian tsunami. *Geophys. Res. Letters* (1998) **25**, No. 14, 2687–2690.
13. F. Imamura and M. M. A. Imteaz, Long waves in two-layers: governing equations and numerical model. *Science of Tsunami Hazards* (1995) **13**, No. 1, 3–24.
14. L. Jiang and P. H. LeBlond, The coupling of a submarine slide and the surface waves which it generates. *J. Geophys. Res.* (1992) **97**, No. C8, 12731–12744.
15. L. Jiang and P. H. LeBlond, Numerical modelling of an underwater Bingham plastic mudslide and the waves which it generates. *J. Geophys. Res.* (1993) **98**, No. C6, 10303–10317.
16. P. J. Lynett and P. L.-F. Liu, A numerical study of the runup generated by three-dimensional landslides. *J. Geophys. Res.* (2005) **110**, No. C03006, doi: 10.1029/2004JC002443.
17. E. Pelinovsky and A. Poplavsky, Simplified model of tsunami generation by submarine landslides. *J. Phys. Chem. Earth* (1996) **21**, No. 12, 13–17.
18. S. Savage and K. Hutter, The motion of a finite mass of granular material down a rough incline. *J. Fluid Mech.* (1989) **199**, 177–215.
19. Yu. I. Shokin, Z. I. Fedotova, G. S. Khakimzyanov, L. B. Chubarov, and S. A. Beizel, Modelling

surfaces waves of generated by a moving landslide with allowance for vertical flow structure. *Russ. J. Numer. Anal. Math. Modelling* (2007) **22**, No. 1, 63–85.

20. S. Tinti, E. Bortolucci, and C. Vannini, A block-based theoretical model suited to gravitational sliding. *Natural Hazards* (1997) **16**, 1–28.
21. P. Watts, Wavemaker curves for tsunamis generated by underwater landslides. *J. Waterway Port Coastal and Ocean Eng.* (1998) **124**, No. 3, 127–137.
22. P. Watts and S. T. Grilli, Underwater landslide shape, motion, deformation, and tsunami generation. In: *Proceedings of the 13th International Offshore and Polar Engineering Conference, Vol. 3*. Honolulu, Hawaii, 2003, pp. 364–371.
23. P. Watts, S. T. Grilli, J. T. Kirby, G. J. Fryer, and D. R. Tappin, Landslide tsunami case studies using a Boussinesq model and a fully nonlinear tsunami generation model. *Natural Hazards and Earth System Sciences* (2003), **3**, No. 5, 391–402.
24. P. Watts, S. T. Grilli, D. Tappin, and G. J. Fryer, Tsunami generation by submarine mass failure. II: Predictive equations and case studies. *J. Waterway Port Coastal and Ocean Engrg.* (2005) **131**, No. 6, 298–310.
25. P. Watts, F. Imamura, and S. T. Grilli, Comparing model simulations of three benchmark tsunami generation cases. *Science of Tsunami Hazards* (2000) **18**, No. 2, 107–123.